

Geometrically induced singular behavior of entanglement

D. Cavalcanti,¹ P. L. Saldanha,² O. Cosme,² F. G. S. L. Brandão,^{3,4} C. H. Monken,² S. Pádua,² M. França Santos,² and M. O. Terra Cunha⁵

¹*ICFO-Institut de Ciències Fotoniques, Mediterranean Technology Park, 08860 Castelldefels (Barcelona), Spain*

²*Departamento de Física, Universidade Federal de Minas Gerais, Caixa Postal 702, 30123-970, Belo Horizonte, MG, Brazil*

³*QOLS, Blackett Laboratory, Imperial College London, London SW7 2BW, UK*

⁴*Institute for Mathematical Sciences, Imperial College London, London SW7 2BW, UK*

⁵*Departamento de Matemática, Universidade Federal de Minas Gerais, Caixa Postal 702, 30123-970, Belo Horizonte, MG, Brazil*

We show that the geometry of the set of quantum states plays a crucial role in the behavior of entanglement in different physical systems. More specifically it is shown that singular points at the border of the set of unentangled states appear as singularities in the dynamics of entanglement of smoothly varying quantum states. We illustrate this result by implementing a photonic parametric down conversion experiment. Moreover, this effect is connected to recently discovered singularities in condensed matter models.

Entanglement, a genuine quantum correlation, plays a crucial role in different physical situations ranging from information processing [1] to quantum many-particle phenomena [2]. Similarly to thermodynamics, smooth variations of controllable parameters which characterize a physical system may lead to singular behavior of entanglement quantifiers. In some cases, in similarity to quantum phases transitions [3], these singularities are attested by abrupt changes in the quantum state describing the system. However, unexpected singularities may appear even when the quantum state varies smoothly [4]. Here we demonstrate how the geometry of the set of unentangled states can be related to singular behavior in physical phenomena. In particular we show that singularities at the boundary of this set can be detected by measuring the amount of entanglement of smoothly varying quantum states.

Entangled states are defined as the states of composed quantum systems which cannot be written as a convex sum of products of density matrices for each composing part [5]. Separable states, on the other hand, admit such a representation and form a convex, closed set with positive volume (for finite dimensional systems) [6]. This set, henceforth designated by S , is a subset of D , the set of all density matrices ($S \subset D$), which is also convex and closed. Therefore, a natural geometric way to quantify entanglement is to see how far - using some definition of distance on the state space - an entangled state is from the set S . This has been carried over for a variety of notions of distance, generating different measures of entanglement [7]. One of these geometric quantifiers is the random robustness, R_R , defined for any state ρ as the minimum s ($s \geq 0$) such that the state

$$\sigma = \frac{\rho + s\pi}{1 + s} \quad (1)$$

is separable ($\pi = I/d$, where I is the identity matrix and d the total dimension of the state space) [8]. The physical

motivation is clear: σ represents a mixture of ρ with the random state π , and $R_R(\rho)$ quantifies how much of this noise must be added to ρ in order to obtain a separable state.

The main result of this Letter is to show that R_R can be used to investigate the shape of the boundary of S , ∂S . The principle is to take an entangled state depending smoothly on one parameter q and compute R_R as a function of q . The one-parameter-dependent density matrices $\rho(q)$ can be seen as a curve in the set of quantum states as shown in Fig. 1. Singularities at ∂S will show up as singularities in $R_R(\rho(q))$. This statement is general for any finite dimension and will be formalized by the contrapositive: if ∂S is non-singular, then $R_R(\rho(q))$ is also non-singular. More precisely:

Proposition 1. *Let D be a closed, convex set. Let $S \subset D$ also be closed and convex, with π a point in the interior of S . If ∂S is a C^m manifold and the states $\rho(q)$ describe a C^m curve in D with no points in the interior of S and obeying the condition that the tangent vector $\rho'(q)$ is never parallel to $\pi - \rho(q)$, then $R_R(\rho(q))$ is also a C^m function.*

One must remember that a manifold is called C^m if it can be parameterized by functions with continuous derivatives up to order m [25]. The reader can change C^m by smooth, in the usual sense of C^∞ , with almost no loss (actually, we use smooth throughout this Letter in the less precise sense of “as regular as necessary”). Other topological remarks before the proof: the fact that S has interior points implies that S and D have the same dimensionality (since there is an open ball of D contained in S), and the proof will use the notion of (topological) cone, which simply means the union of all segments from a given point V to each point of a given set A : this is called the cone of A with vertex V .

Proof: The geometrical situation leads to the cone, given by $(p, q) \mapsto p\pi + (1-p)\rho(q)$, $p \in [0, 1]$. The condition

on the tangent vector (together with the fact that π is interior to S , while $\rho(q)$ has no point in this interior) is sufficient for this cone to be C^m , except at the vertex π , at least locally in q .

As S is bounded and convex, and π is in its interior, every straight line from π crosses ∂S exactly once. As $\rho(q)$ has no point in the interior of S , this crossing always happens for $0 \leq p < 1$. Denote this crossing value by $p_c(q)$. The curve $q \mapsto p_c(q)\pi + (1 - p_c(q))\rho(q)$ is C^m , implying p_c is a C^m function of q .

The random robustness is given by $R_R(\rho(q)) = \frac{p_c}{1-p_c}$. As $p_c < 1$, we also obtain that R_R is a C^m function of q . \square

We insist on the interpretation: Proposition 1 means that any singularity in R_R for a well chosen path $\rho(q)$ reflects singularities in ∂S .

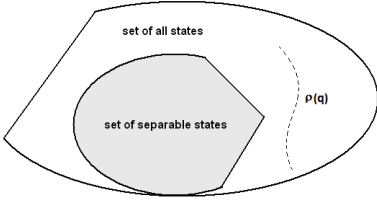


FIG. 1: **State space.** The dotted line represents the path $\rho(q)$ followed by ρ when parameter q is changed. It is worth noting that S can present singular points in its shape and to remember that the “true” picture is much subtler, given the large dimensionality of even the simplest example [9].

From this point on, we study the situation for two qubits, which is related to the performed experiment described here. In this case, Ref. [10] shows that the Random Robustness is proportional to the Negativity ($\mathcal{N}(\rho)$) [11], given by the absolute value of the sum of the negative eigenvalues of the partial transposed state. The negativity is a monotone under local operations and classical communication [12] and has the operational interpretation of a cost function under a certain class of operations [13, 14].

At the same time, entanglement can be measured with the help of entanglement witnesses [15]. These are Hermitian operators with positive mean value for all separable states, but with a negative mean value for some entangled states [16]. In fact, many geometrical entanglement quantifiers are directly related to witness operators [17]. In the particular case of two qubits [26], we have that for every entangled state ρ [10],

$$2\mathcal{N}(\rho) = R_R(\rho) = -2 \min_{W \in \mathcal{W}} \text{Tr}(W\rho), \quad (2)$$

where \mathcal{W} is the set of entanglement witnesses W with $\text{Tr} W = 2$.

At this point we might ask some natural questions. Is there in fact any singularity in the shape of S ? In the affirmative case, does this singularity appear in any

physical setup? We proceed to answer positively both questions by showing physical processes where a singularity in ∂S is revealed by monitoring the entanglement of a given system.

First, let us consider a general system of four qubits a, b, A , and B , subject to the following Hamiltonian [19]:

$$H = H^{aA} + H^{bB}, \quad (3)$$

where

$$H^{\mu\nu} = \frac{\omega}{2}\sigma_z^\mu + \frac{\omega}{2}\sigma_z^\nu + \frac{g}{2}(\sigma_-^\mu\sigma_+^\nu + \sigma_+^\mu\sigma_-^\nu). \quad (4)$$

Here $\sigma_+ = (\sigma_x + i\sigma_y)/2$ and $\sigma_- = (\sigma_x - i\sigma_y)/2$, where σ_x, σ_y and σ_z are the usual Pauli matrices. This scenario can be realized in many systems, like cavity QED [20], trapped ions [21], and quantum dots [22]. We set the initial state to be $|\psi(t=0)\rangle = |\Phi_+\rangle_{ab} \otimes |\Psi_+\rangle_{AB}$, where qubits ab are in the Bell state $|\Phi_+\rangle = (|00\rangle + |11\rangle)/\sqrt{2}$ and qubits AB are in the orthogonal Bell state $|\Psi_+\rangle = (|01\rangle + |10\rangle)/\sqrt{2}$. Hamiltonian (3) induces a swapping process which leads (in the interaction picture) to the following temporal evolution for the subsystem AB , obtained by tracing out the subsystem ab :

$$\rho_{AB}(t) = q|\Psi_+\rangle\langle\Psi_+| + (1-q)|\Phi_+\rangle\langle\Phi_+|, \quad (5)$$

where $q = \cos^2(gt)$. For this state the negativity reads

$$\mathcal{N}(\rho_{AB}(t)) = \max\{1 - 2q, 2q - 1\} = |1 - 2q|. \quad (6)$$

This function presents a singularity for $q = 0.5$ ($gt = n\pi/4$, with n odd) signaling then a singularity at ∂S .

Another physical process which also produces the family of states (5) is the following simple quantum communication task: Alice prepares a Bell state $|\Phi_+\rangle$ and sends one qubit to Bob through a quantum channel; if this channel has a probability q of introducing a bit flip, and $1 - q$ of no error at all, the state (5) is the output of the process [27].

To illustrate the dynamics given by Eq. (5), we have performed an optical experiment, shown in Fig. 2. In our experiment, twin photons maximally entangled in polarization are generated in a non-linear crystal [23] and sent to an unbalanced Michelson interferometer, which is used to simulate the channel described above. The experiment works as follows: we produce a two-photon $|\Psi_+\rangle$ state, send one of the photons directly to the detection stage, and the other to the (unbalanced) interferometer. One of the arms of this interferometer does not change the polarization of the photon, and if the photon went through this path the two photons would be detected in $|\Psi_+\rangle$. However if the photon went through the other path its polarization would be rotated in such a way that the final two-photon state would become $|\Phi_+\rangle$. We have made a tomographic characterization of the photonic states corresponding to these two extremal points.

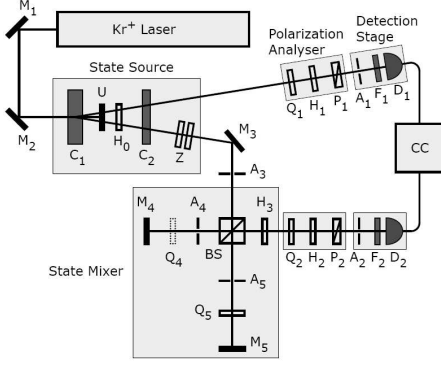


FIG. 2: Experimental setup: The state source is composed by a 2mm-thick BBO (β -BaB₂O₄) nonlinear crystal (C₁) pumped by a cw krypton laser operating at 413nm, generating photon pairs at 826nm by type II spontaneous parametric down-conversion. Crystal C₁ is cut and oriented to generate either one of the polarization entangled Bell states $|\Psi_{-}\rangle$ or $|\Psi_{+}\rangle$. Walk-off and phase compensation is provided by the half-wave plate H₀ followed by a 1mm-thick BBO crystal (C₂) [23], together with two 1mm-thick crystalline quartz plates (Z) inserted in one of the down-converted photon paths. The unconverted laser beam transmitted by crystal C₁ is discarded by means of a dichroic mirror (U). The detection stages are composed by photon counting diode modules D₁ and D₂, preceded by 8nm FWHM interference filters F₁ and F₂ centered at 825nm, and by circular apertures A₁ of 1.6mm \emptyset and A₂ of 3.0mm \emptyset . Single and coincidence counts with 5ns resolving time are registered by a computer controlled electronic module (CC). Polarization analyzers are composed by quarter-wave plates Q₁ and Q₂, half-wave plates H₁ and H₂, followed by polarizing cubes P₁ and P₂. The State Source produces state $|\Psi_{-}\rangle$. For each pair, the photon emerging in the upper path goes straight to the polarization analyzer and to the detection stage 1. The lower path photon is directed by mirror M₃ through the circular aperture A₃ into the state mixer (an unbalanced Michelson interferometer), composed by the beam splitter BS, mirrors M₄ and M₅, quarter-wave plates Q₄ and Q₅, variable circular apertures A₄ and A₅, and by the half-wave plate H₃, whose purpose is to compensate for an unwanted slight polarization rotation caused by the beam splitter. The quarter-wave plate Q₄ is switched off which means that if the lower photon follows path labeled 4, there is no change to its polarization and the half-wave plate H₃ changes the state to $|\Psi_{+}\rangle$. On the other hand, if the lower photon follows path labeled 5, Q₅ is oriented with the fast axis at 45° in order to flip its polarization. The path length difference, 130mm, is much larger than the coherence length of the down-converted fields, ensuring an incoherent recombination at BS. The pair detected by CC is in state $q|\Psi_{+}\rangle\langle\Psi_{+}| + (1-q)|\Phi_{+}\rangle\langle\Phi_{+}|$ where q is defined by the relative sizes of apertures A₄ and A₅.

The reconstructed density matrices are displayed in Fig. 3. These two possibilities are then incoherently recombined, thus allowing the preparation of state (5). Each preparation yields a different value for q with the corre-

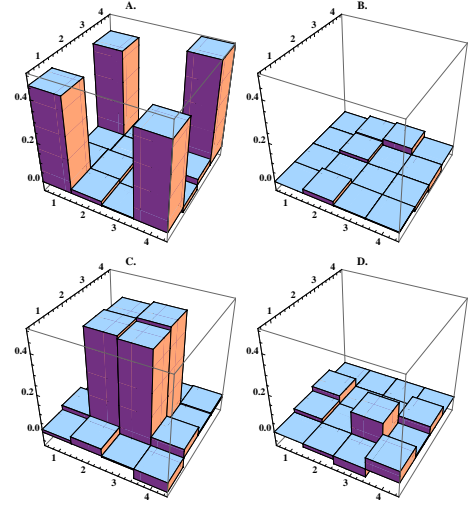


FIG. 3: (Color online) The reconstructed density matrices corresponding (ideally) to the states $|\Phi_{+}\rangle$ (A. real and B. imaginary parts) and $|\Psi_{+}\rangle$ (C. real and D. imaginary parts). The attained fidelity for these states are, respectively, $F_{\Phi_{+}} \equiv \langle\Phi_{+}|\rho|\Phi_{+}\rangle \approx (92 \pm 3)\%$ and $F_{\Psi_{+}} \equiv \langle\Psi_{+}|\rho|\Psi_{+}\rangle \approx (96 \pm 3)\%$.

sponding optimal witness given by

$$W_{opt} = \begin{cases} I - 2|\Phi_{+}\rangle\langle\Phi_{+}|, & \text{for } 0 \leq q \leq 1/2, \\ I - 2|\Psi_{+}\rangle\langle\Psi_{+}|, & \text{for } 1/2 \leq q \leq 1. \end{cases} \quad (7)$$

For the family of generated states these two observables are the only candidates of optimal entanglement witnesses, so they are the only ones to be measured. In a more general situation, if less is known about the prepared state, much more candidate witnesses should be measured. The results are displayed in Fig. 4. The blue curve in the figure shows the witnessed negativity measurement and its edge indicates the existence of singularities at ∂S . This experimental result shows the abrupt change in the optimal witness at the value $q = \frac{1}{2}$, which heralds the singularity in ∂S . As a proof of principles, each operator W is measured for the whole range of q , which yields the points below zero in Fig. 4. Note that the singularity occurs exactly for $R_R = 0$ ($q = 1/2$). According to our geometrical interpretation, this means the path followed by the parameterized state $\rho(q)$ touches the border of S . This result must not be a surprise, since it is well known that in the tetrahedron generated by the Bell states (which we access in our experiment) the separable states form an inscribed octahedron [24].

The geometrical properties of entanglement discussed here give new insight into singularities found recently in the entanglement of condensed matter systems. Striking examples, dealing with entanglement properties of certain spin- $\frac{1}{2}$ models subjected to a transverse magnetic field h , are described in Refs. [4]. In these works, the two-qubit reduced state shows a singularity in entanglement for a particular field value h_f far from the critical field of the respective model. As correlation functions,

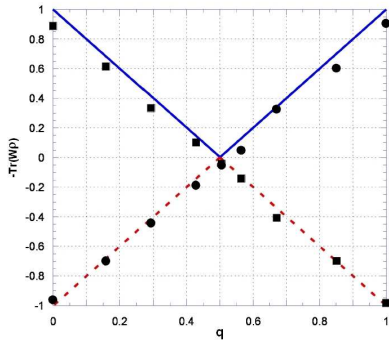


FIG. 4: (Color online) Measurement of the mean value of both operators described in (7) for the full range $0 \leq q \leq 1$. Each W is expanded as a linear combination of products of local operators which are then measured independently. The blue continuous line corresponds to the theoretical value of $\mathcal{N}(\rho(q))$ for the state $\rho(q) = q|\Psi_+\rangle\langle\Psi_+| + (1-q)|\Phi_+\rangle\langle\Phi_+|$. Note that each W only witnesses entanglement for a restricted range of q values as predicted by the theory. The local singularity of ∂S is evidenced by the abrupt change of optimal W . Experimental errors are within the dots' sizes.

ground state energy, and even reduced density matrices are all smooth at h_f , there was no clear origin for these singularities. Our results offer an explanation by interpreting the non-analyticities exhibited by entanglement as a consequence of geometric singularities at ∂S [28].

As previously mentioned, R_R can be used to probe ∂S in any finite dimensional system. For example, a previous work showed a singular behavior of R_R in three qubits systems [10]. Within the scope of our paper, we can interpret it as originated by a singularity at the border of the respective separable set. Note, however, that in this case, due to the higher dimensionality of the system, the singularity at ∂S occurs in the interior of D , with R_R showing a singularity at a positive value.

To sum up, we have presented a method for probing the shape of the set of separable states. Singularities in this set were found and connected to non-analytical behavior of entanglement in different physical systems. It is an interesting open question to find physical implications of such singularities.

We acknowledge discussions with A. Acín, A. Sen(De), J. Wehr, E. Rico, G. Palacios, V. Vedral, and J. Dunningham and funding from CNPq, Fapemig, PRPq-UFMG, and Brazilian Millenium Institute for Quantum Information.

[1] A.K. Ekert, Phys. Rev. Lett. **67**, 661 (1991).
[2] L. Amico, R. Fazio, A. Osterloh, and V. Vedral, arXiv:quant-ph/0703044.
[3] T. J. Osborne and M. A. Nielsen, Phys. Rev. A **66**, 032110 (2002); A. Osterloh, L. Amico, G. Falci, and R.

Fazio, Nature **416**, 608 (2002).
[4] A. Osterloh, G. Palacios, and S. Montangero, Phys. Rev. Lett. **97**, 257201 (2006); T. Roscilde *et al.*, *ibid* **93**, 167203 (2004); *ibid* **94**, 147208 (2005).
[5] R. F. Werner, Phys. Rev. A **40**, 4277 (1989).
[6] K. Życzkowski, P. Horodecki, A. Sanpera, and M. Lewenstein, Phys. Rev. A **58**, 883 (1998).
[7] R. Horodecki, P. Horodecki, M. Horodecki, and K. Horodecki, arXiv:quant-ph/0702225; M. B. Plenio and S. Virmani, Quant. Inf. Comp. **7**, 1 (2007).
[8] G. Vidal and R. Tarrach, Phys. Rev. A **59**, 141 (1999).
[9] I. Bengtsson and K. Życzkowski, *Geometry of Quantum States: An Introduction to Quantum Entanglement*. (Cambridge Univ. Press, Cambridge, 2006).
[10] F. G. S. L. Brandão and R. O. Vianna, Int. J. Quant. Inf. **4**, 331 (2006).
[11] G. Vidal and R. F. Werner, Phys. Rev. A **65**, 032314 (2002). Note that in our work Negativity for two qubits runs from 0 to 1.
[12] J. Eisert, PhD thesis University of Potsdam, arxiv quant-ph/0610253.
[13] K. Audenaert, M. B. Plenio, and J. Eisert, Phys. Rev. Lett. **90**, 027901 (2003).
[14] S. Ishizaka, Phys. Rev. A **69**, 020301(R) (2004).
[15] M. Barbieri *et al.*, Phys. Rev. Lett. **91**, 227901 (2003); O. Gühne *et al.*, J. Mod. Opt. **50**, 1079 (2003); M. Bourennane *et al.*, Phys. Rev. Lett. **92**, 087902 (2004); D. Cavalcanti and M. O. Terra Cunha, App. Phys. Lett. **89**, 084102 (2006); K. Audenaert and M. B. Plenio, New J. Phys. **8**, 266 (2006); O. Gühne, M. Reimpell, and R. F. Werner, Phys. Rev. Lett. **98**, 110502 (2007); J. Eisert, F. G. S. L. Brandão, and K. M. R. Audenaert, New J. Phys. **9**, 46 (2007).
[16] M. Horodecki, P. Horodecki, and R. Horodecki, Phys. Lett. A **223**, 1 (1996); B. M. Terhal, Phys. Lett. A **271**, 319 (2000).
[17] F. G. S. L. Brandão, Phys. Rev. A **72**, 022310 (2005).
[18] M. Lewenstein, B. Kraus, J. I. Cirac, and P. Horodecki, Phys. Rev. A **62**, 052310 (2000).
[19] D. Cavalcanti *et al.*, Phys. Rev. A **74**, 042328 (2006).
[20] J. M. Raymond, M. Brune, and S. Haroche, Rev. Mod. Phys. **73**, 565 (2001).
[21] M. D. Barrett *et al.*, Nature **429**, 737 (2004).
[22] W. D. Oliver, F. Yamaguchi, and Y. Yamamoto, Phys. Rev. Lett. **88**, 037901 (2002).
[23] P. G. Kwiat *et al.*, Phys. Rev. Lett. **75**, 4337 (1995).
[24] R. Horodecki and M. Horodecki, Phys. Rev. A **54**, 1838 (1996).
[25] M. Spivak, Calculus on Manifolds: A modern approach to classical theorems of advanced calculus (W.A. Benjamin, New York, 1965).
[26] An optimal entanglement witness W_{opt} satisfying (2) is proportional to the partial transposition of the projector over the eigenspace of the negative eigenvalue of ρ^{T_2} , where ρ^{T_2} denotes the partial transposition of ρ [18].
[27] The simplest way of drawing the complete line represented by Eq. (5) is to consider three different initial conditions: from $|\Phi_+\rangle$ one obtains $q \in [0, 1/2]$, from $|\Psi_+\rangle$, $q \in (1/2, 1]$, and $q = 1/2$ is a fixed point of this dynamical system.
[28] Although the results of Refs. [4] were obtained in terms of the concurrence, a completely analogous result holds for the negativity as well.